7. From Radiation Fields to Atmospheric Concentrations – Retrieval of Geophysical Parameters

The challenging task in spaceborne remote sensing of the atmospheric composition is the quantitative derivation of the constituent distributions – trace gases, aerosol, clouds – from the measured top-of-the-atmosphere spectral radiance or Earth spectral reflectance data. The source of radiation for passive remote sounding of the atmosphere by SCIAMACHY in the UV-SWIR regions is the sun. The absorption and scattering characteristics of the Earth's atmosphere can be determined by comparing the radiance reflected from and scattered by the atmosphere to the sensor with the extraterrestrial solar irradiance. The ratio of the radiance to irradiance, the Earth reflectance spectrum, contains the information relevant for determining the atmospheric composition. A quantitative analysis requires:

- spectra of high spectral and radiometric quality,
- an accurate modelling of the radiative transfer of the solar photons through the atmosphere to the sensor,
- techniques to relate the measured top-of-the-atmosphere spectra to the constituent properties (usually referred to as *Inversion Methods*).

The retrieval of information on atmospheric trace gases relies on the knowledge of the absorption, emission and scattering of electromagnetic radiation in the atmosphere. In the UV, VIS, NIR and SWIR spectral ranges, the radiative transfer through the atmosphere is affected by (see fig. 7-1):

- scattering by air molecules (Rayleigh-, Raman scattering),
- scattering and absorption by aerosol and cloud particles (Mie-scattering),
- absorption and emission by trace gases,
- refraction due to the density gradient in the atmosphere,
- surface reflection.

These are the processes which must be quantitatively taken into account when retrieving atmospheric geophysical parameters from SCIAMACHY measurements.

Trace gases usually exhibit characteristic fingerprint spectra in emission or absorption, originating from:

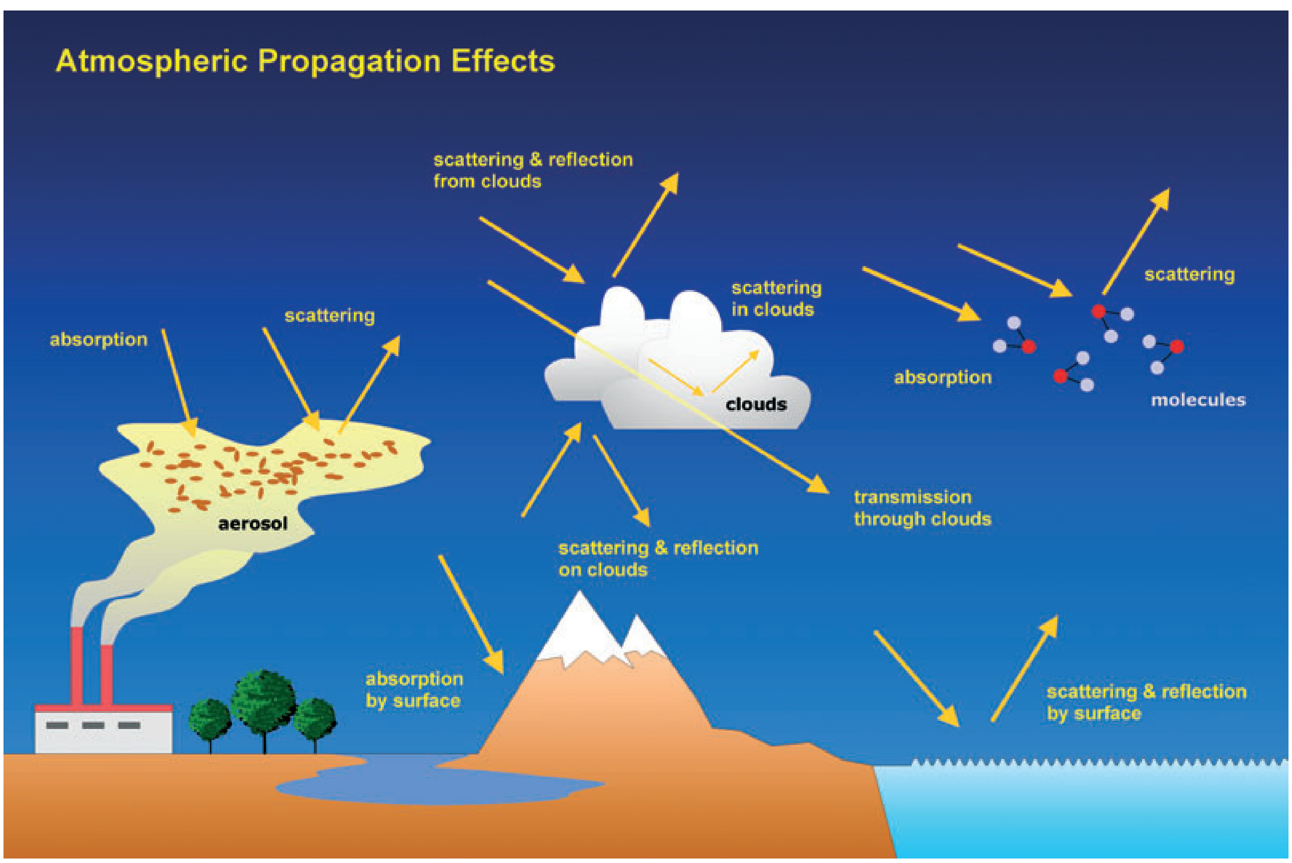

Fig. 7-1: Scheme of the relevant interactions of solar light with the Earth's atmosphere and surface. (graphics: DLR-IMF)

- rotational transitions: primarily observed in the far infrared and microwave spectral regions,
- vibrational-rotational transitions: can be measured in the infrared,
- electronic transitions: mainly detected in the UV, VIS and NIR spectral regions.

SCIAMACHY with its wide spectral coverage from the UV to the SWIR is detecting trace gases mainly via their electronic transition spectra.

7.1 Radiative Transfer in the Earth's Atmosphere

An important tool to simulate changes in the solar radiation due to atmospheric scattering and absorption processes are radiative transfer models, also referred to as *Forward Models*. They provide the synthetic radiances, as they would be measured by the sensor, for a specified state of the atmosphere. These models are an important part of any retrieval process. Considering the entire atmosphere, one usually talks about the radiation field, which describes the angular and spatial distribution of the radiation in the atmosphere.

The radiation field in the atmosphere is commonly characterised by its intensity which is defined as the flux of energy in a given direction per second per unit wavelength range per unit solid angle per unit area perpendicular to the given direction *(Liou 2002)*. All interactions between the radiation and the atmosphere are classified either as extinction or as emission. The two processes are distinguished by the sign of the change of the radiation intensity as a result of the interaction. *Extinction* refers to any process which reduces the intensity in the direction under consideration and therefore includes absorption as well as scattering processes from the original direction into other directions. *Emission* refers to any process which increases the intensity in the direction under consideration and thus includes scattering into the beam from other directions, as well as thermal or other emission processes within the volume. In the description of radiative transfer presented here we neglect the polarisation state of light for reasons of simplicity. However, we note that polarisation is important for SCIAMACHY for two reasons, namely in order to

- accurately simulate radiances in the UV and VIS
- account for the polarisation sensitivity of the instrument when determining the true radiance (see discussion in chapter 5)

The general form of the radiative transfer equation describes all the processes which the radiance undergoes as a result of its interaction with a medium, taking energy conservation into account. It has the form (equ. 7-1)

$$\frac{\mathrm{d}I}{\mathrm{d}s} = -\alpha \cdot (I - J)$$

where I is the intensity of the radiation in a given direction, α is the extinction coefficient describing the fraction of the energy which is removed from the original beam and J is the source function which describes the energy emitted by the volume element, i.e., the increase of the intensity, I, in the original direction.

If the energy of the radiance travelling in a certain direction through the atmosphere can only be increased due to the scattering processes – as is the case for the spectral range covered by SCIAMACHY – the source function depends on the intensity falling on the elementary volume from all directions (equ. 7-2)

$$J = \frac{\omega}{4\pi} \int p(\gamma)\, I\, \mathrm{d}\Omega$$

with γ being the scattering angle, i.e. the angle between the directions of the incident and scattered radiation, and ω is the single scattering albedo representing the probability that a photon which interacts with a volume element will be scattered rather than absorbed. The term $p(\gamma)\,\mathrm{d}\Omega/4\pi$ denotes the probability that the radiation is scattered into a solid angle $\mathrm{d}\Omega$ about a direction forming an angle γ with the direction of the incident radiation and the quantity $p(\gamma)$ is called the phase function.

The total radiation field can be split into two components: the direct radiation, I_{dir}, which is never scattered in the atmosphere or reflected from the Earth's surface and the diffuse radiation, I_{dif}, which is scattered or reflected at least once. Since there is no relevant process in the atmosphere which increases the intensity of the direct solar radiation, the radiative transfer equation for the direct radiation leads to the homogeneous differential equation (equ. 7-3)

$$\frac{\mathrm{d}I_{dir}}{\mathrm{d}s} = -\alpha \cdot I_{dir}$$

with a solution described by the Lambert-Beer's Law (equ. 7-4)

$$I_{dir} = I_{irr} \exp\left(-\int \alpha(s)\,\mathrm{d}s\right)$$

with I_{irr} being the solar irradiance and the integral $\int\alpha(s)\mathrm{d}s$ along the photon path defining the *optical depth* τ. Integration is performed along the direct solar beam from the surface to the top of the atmosphere. This equation describes the attenuation of the direct solar or lunar light travelling through the atmosphere. Thus the direct component (equ. 7-4) simulates the radiative transfer when for example directly viewing the sun or the moon. Therefore, it describes SCIAMACHY measurements in occultation geometry.

If the scattering processes in the atmosphere are non-negligible – as for SCIAMACHY nadir and limb measurements – the diffuse component has to be considered in addition to the direct one. This leads to the standard radiative transfer equation for the diffuse component for a plane-parallel atmosphere (equ. 7-5)

$$\frac{\mathrm{d}I_{dif}}{\mathrm{d}s} + \alpha\cdot\left(I_{dif} - \frac{\omega}{4\pi}\int p(\gamma)\,I_{dif}\,\mathrm{d}\Omega\right) = \frac{\omega}{4\pi}\,p(\gamma_0)\,I_{irr}\exp\left(-\int\alpha(s)\,\mathrm{d}s\right)$$

where γ_0 denotes the scattering angle between the direct solar beam and the direction of observation.

Scattering occurs by molecules and various types of aerosols and clouds. Molecular scattering cross-sections are characterised by the Rayleigh (λ^{-4}) law, with aerosol scattering typically showing a much less pronounced dependence on wavelength (about λ^{-1}). Molecular scattering dominates in the UV with aerosols replacing molecules as the major source of scattered light in the VIS and NIR range (see fig. 7-3). The molecular scattering consists of two parts: the elastic Rayleigh component which accounts for 96% of scattering events and the 4% inelastic rotational Raman component, which is considered responsible for the so called *Ring* effect ('filling in' of solar Fraunhofer lines in the Earthshine spectra). Further details on atmospheric radiative transfer can be found in e.g. *Liou (2002)*.

Direct and diffuse radiation are attributed to different light paths. Equations 7-4 and 7-5 need to be solved employing standard methods *(Lenoble 1985)*. I_{dir} and I_{dif} must be added to describe the radiative transfer for the SCIAMACHY nadir geometry for not too large solar zenith angles (SZA). As an example, figure 7-2 shows the solar irradiance spectrum and the backscattered radiance at the top of the atmosphere. When SCIAMACHY nadir radiances at high SZA > 75° are simulated, the sphericity of the atmosphere must be taken into account in a pseudo-spherical approximation for the direct solar beam. For simulating SCIAMACHY limb radiances both the direct and the diffuse solar beam have to be treated in a spherical atmosphere, including refraction. The numerical solution of the radiative transfer equation is then accomplished by an iterative approach *(Rozanov et al. 2001)*. Depending on the scientific application, several radiative transfer models are used in the SCIAMACHY data analysis. They include GOMETRAN *(Rozanov et al. 1998)*, LIDORT *(Spurr et al. 2001)*, DAK *(Stammes 2001)*, SCIARAYS *(Kaiser and Burrows 2003)* and SCIATRAN 2.0 *(Rozanov et al. 2005a)*. These radiative transfer models are not only able simulating the radiance measured by SCIAMACHY, but they are also optimised to deliver additional parameters to quantify the geophysical parameters of interest. One of these parameters is the *Weighting Function*. This function is the derivative of the modelled radiance with respect to the model parameter, and describes how sensitive the radiance changes are when the parameters are modified. Another important quantity to be delivered by radiative transfer models is the Airmass Factor (AMF, see chapter 7.2) which is a measure for the photon path in the atmosphere.

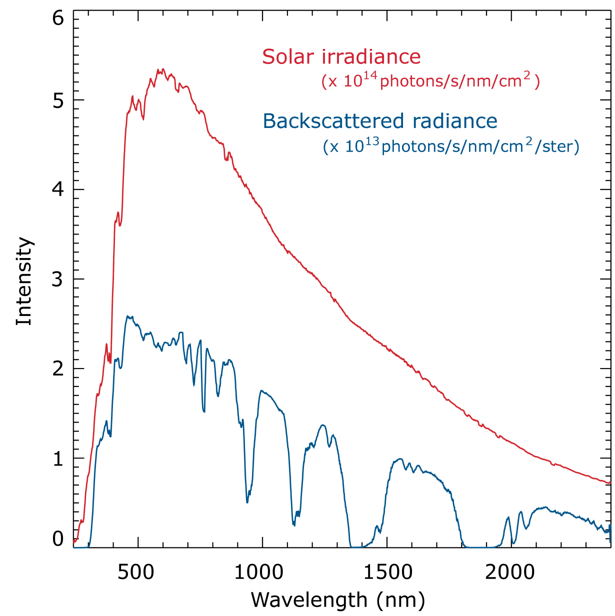

Fig. 7-2: The solar irradiance spectrum (red) and Earth radiance spectrum (blue) with a shape modified by absorption of trace gases and scattering in the atmosphere. (graphics: IUP-IFE, University of Bremen)

7.2 Nadir Retrieval Schemes of DOAS-type

Many molecules of atmospheric relevance have structured absorption spectra in the UV-VIS spectral range (fig. 7-3). These can be used to determine the total atmospheric amount of the species from remote sensing measurements of scattered sunlight using the DOAS method. This powerful retrieval technique was originally developed for ground-based measurements using artificial light sources or scattered sunlight (*Solomon et al. 1987*, *Platt 1994*) but has successfully been adapted to nadir measurements from GOME (*Burrows et al. 1999* and references therein). Two main ideas form the basis of the DOAS approach (see also fig. 7-4):

- the isolation of the high frequency structures of molecular absorbers from broad band scattering features (Rayleigh, Mie) by a high pass filter,
- the separation of spectroscopic retrievals and radiative transfer calculations.

The first step of the data analysis consists of determining the total amount of absorption and scattering by dividing the Earthshine radiance by the direct solar irradiance. The latter provides the absorption free background. The molecular absorption cross section together with a polynomial is then fitted to the logarithm of this ratio, yielding the trace gas concentration along the light path (*slant column concentration*). Fig. 7-5 depicts a typical fit for NO_2. Finally, the average light path through the atmosphere is calculated using a radiative transfer model. The light path is often expressed as airmass factor which is the light path enhancement factor relative to a vertical transection of the atmosphere. Based on the AMF

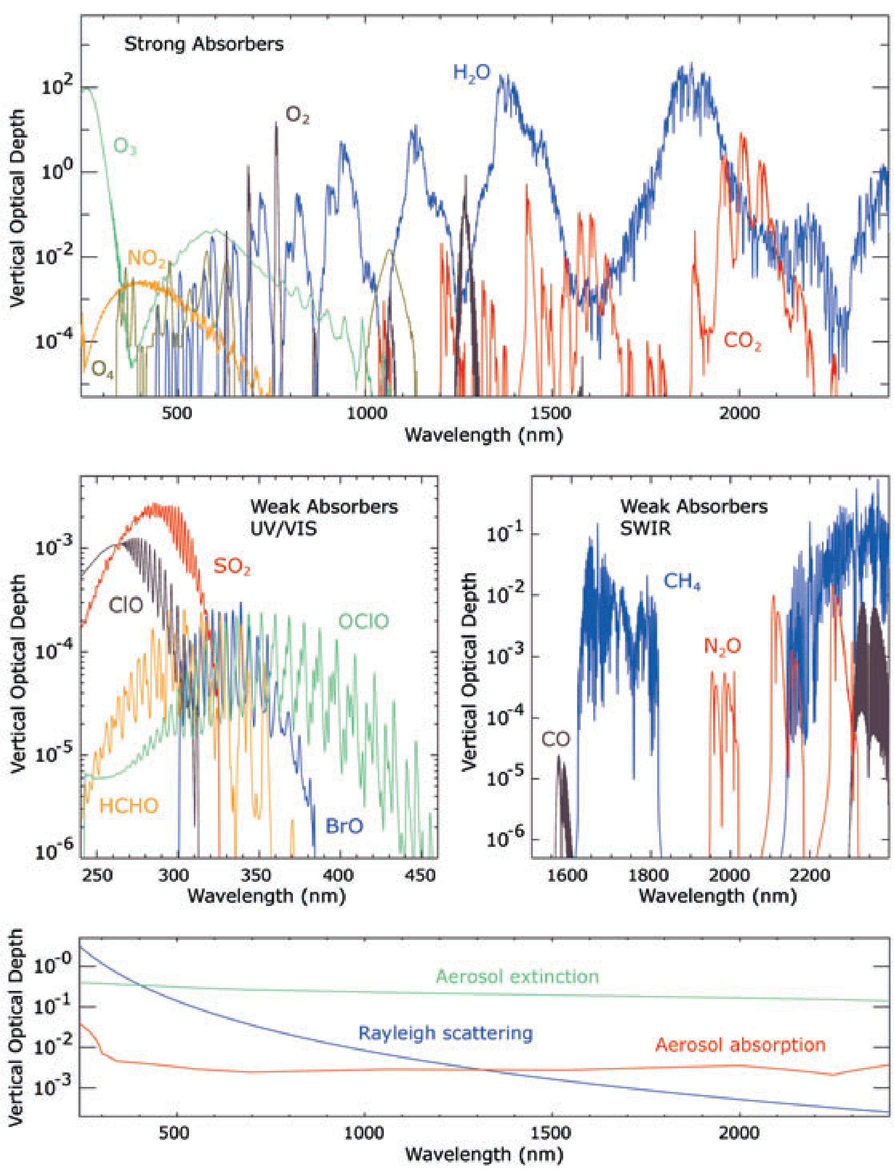

Fig. 7-3: Simulated vertical optical depth of the targeted constituents to be observed at 55° N around 10 a.m. The strong absorbers are plotted in the upper part and the relevant weak absorbers in the middle part. In the lower part the vertical optical depth due to Rayleigh scattering, aerosol extinction and absorption is given. Note the large dynamic range of the differential absorption structures used for retrieval of the constituents. (graphics: IUP-IFE, University of Bremen)

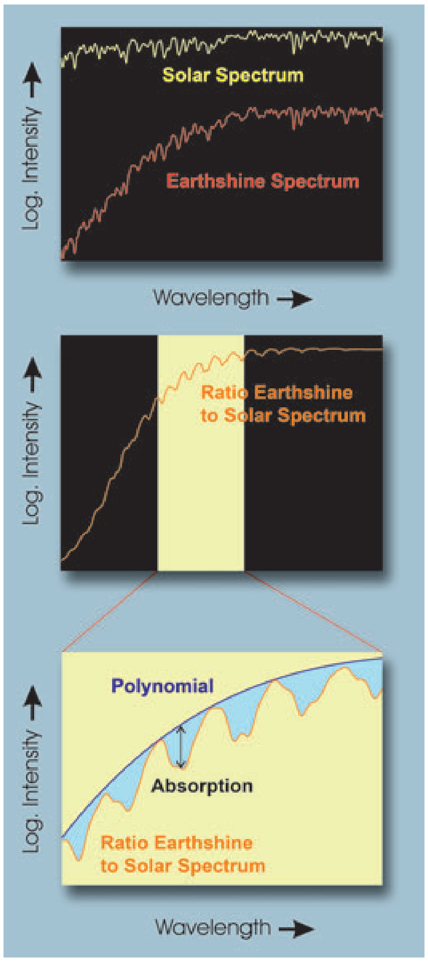

Fig. 7-4: The main steps of the DOAS retrieval. For further details see the text. (graphics: IUP-IFE, University of Bremen)

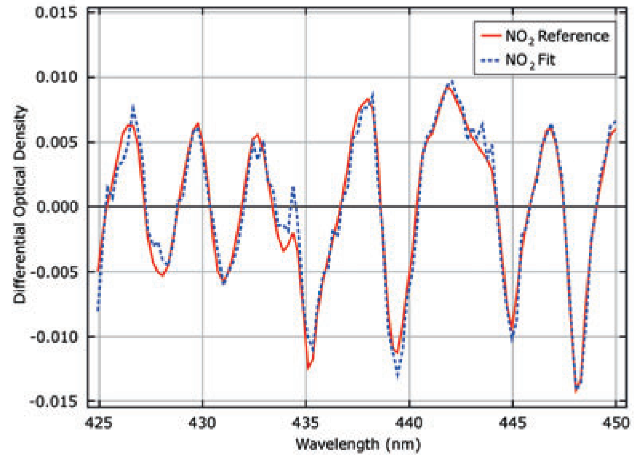

Fig. 7-5: Typical SCIAMACHY NO_2 fit results from a measurement over a polluted area in China on January 15th, 2006. The red line is the scaled NO_2 laboratory cross-section, the dashed blue line the result of the fit after subtraction of all contributions with the exception of NO_2. (graphics: IUP-IFE, University of Bremen)

the vertical column concentration of the absorber may finally be calculated. Obviously clouds drastically modify the light path through the atmosphere and need to be properly taken into account when calculating the AMF (see chapter 7.3). The most important cloud parameter is the cloud fraction, as fractional cloudiness blocks the light path to atmospheric layers below the cloud. Using the DOAS algorithm, atmospheric columns of a number of species can be determined, including O_3, NO_2, SO_2, HCHO, BrO, and OClO *(Burrows et al. 1999, Borell et al. 2003)*.

One limitation of the classical DOAS technique is the assumption that the atmosphere is optically thin in the wavelength region of interest. In addition, 'line-absorbers' such as H_2O, O_2, CO, CO_2 and CH_4 usually cannot be retrieved precisely by standard DOAS algorithms because their strong absorption also depends on pressure, temperature and wavelength and in addition their spectra are often not fully spectrally resolved by SCIAMACHY. To overcome these drawbacks several DOAS-type techniques were developed to account for such effects and to permit successful retrievals of the trace gas species. They are for example the WFM-DOAS *(Buchwitz et al. 2000, de Beek et al. 2006)*, AMC-DOAS *(Noël et al. 2004)*, TOSOMI *(Eskes et al. 2005)*, SDOAS *(Van Roozendael et al. 2006)*, IMAP *(Frankenberg et al. 2005a, 2005b)* and IMLM *(Houweling et al. 2005)*. Figure 7-6 illustrates an example of one day of ozone columns derived from nadir observations with one of these schemes, the TOSOMI algorithm. Table 7-1 summarises the DOAS-type retrieval algorithms as applied to SCIAMACHY data and references to it.

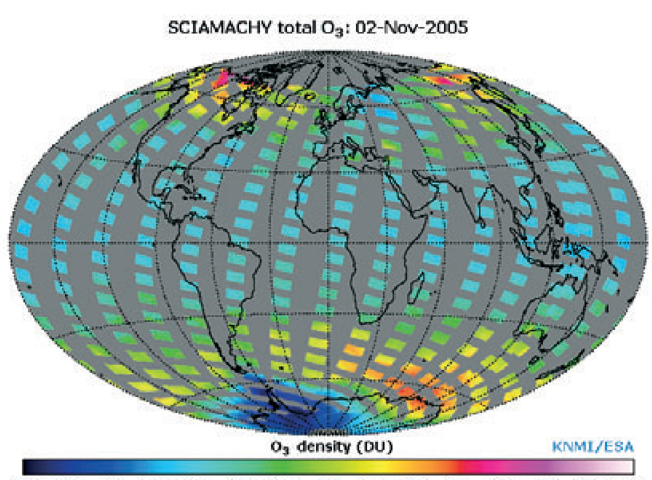

Fig. 7-6: One day of total ozone densities obtained with the TOSOMI algorithm. (image: KNMI/ESA)

Parameter	***Spectral Window (nm)***	***Layer***	***Quantity (column)***	***Retrieval Algorithm***	***Retrieval Algorithm Reference***
O_3	325 – 335	troposphere, stratosphere	total	operational WFM-DOAS TOSOMI SDOAS	*Spurr 2000* *Weber et al. 2005* *Eskes et al. 2005* *Van Roozendael et al. 2006*
NO_2	425-450	troposphere, stratosphere	total, tropospheric	operational DOAS SDOAS	*Spurr 2000* *Richter et al. 2005* *Van Roozendael et al. 2006*
BrO	335-347(55)	troposphere, stratosphere	total	DOAS	
SO_2	315-327	troposphere	total	DOAS	
HCHO	335-347(55)	troposphere	total	DOAS	
OClO	365-389	stratosphere	total	DOAS	
H_2O	688-700	troposphere	total	AMC-DOAS	*Noël et al. 2004*
CO	2321(24)-2335	troposphere	total	WFM-DOAS IMLM IMAP	*de Beek et al. 2006* *de Laat et al. 2006* *Frankenberg et al. 2005b*
CH_4	1627(30)-1671	troposphere	total	WFM-DOAS IMLM IMAP	*de Beek et al. 2006* *Gloudemans et al. 2005* *Frankenberg et al. 2005a*
CO_2	1558(63)-1594(85)	troposphere	total	WFM-DOAS IMLM IMAP	*de Beek et al. 2006* *Houweling et al. 2005* *Frankenberg et al. 2005a*

Table 7-1: Atmospheric geophysical parameters and retrieval algorithms – nadir trace gases.

7.3 Cloud and Aerosol Parameter Retrieval

The primary scientific objective of SCIAMACHY is the measurement of atmospheric trace gases in both the troposphere and stratosphere. However, clouds residing in the troposphere do interfere with the retrievals from SCIAMACHY measurements mainly by the shielding and albedo effects. Similarly, tropospheric and/or stratospheric aerosol interferes with the trace gas retrieval, as it alters the light path. Therefore, there is a clear need for cloud and aerosol information. In addition, cloud information from SCIAMACHY will also provide relevant data for cloud research.

In the UV, VIS and NIR spectral regions the solar radiation is strongly scattered by clouds and aerosol, thereby modifying the Earth reflectance spectrum. The presence of clouds and aerosol and their properties can therefore be determined by analysing the top-of-atmosphere reflection function R. It is defined as (equ. 7-6)

$$R = \frac{\pi \cdot I_{dif}}{\mu_0 \cdot I_{irr}}$$

where μ_0 is the cosine of the solar zenith angle, I_{irr} is the solar irradiance and I_{dif} is the scattered and reflected light in the direction towards the satellite sensor.

Prerequisites for high quality information about aerosol and clouds are high spatial resolution and high calibration accuracy of the reflectance measurements. Typical reflectance spectra for various cloud and surface conditions are shown in fig. 7-7. Various algorithms are required to determine cloud and aerosol properties from SCIAMACHY data. For a summary the reader is referred to table 7-2.

Cloud Parameters

For SCIAMACHY information on cloud parameters are of twofold importance. Firstly, cloud parameters such as cloud fraction, top pressure (or height) and

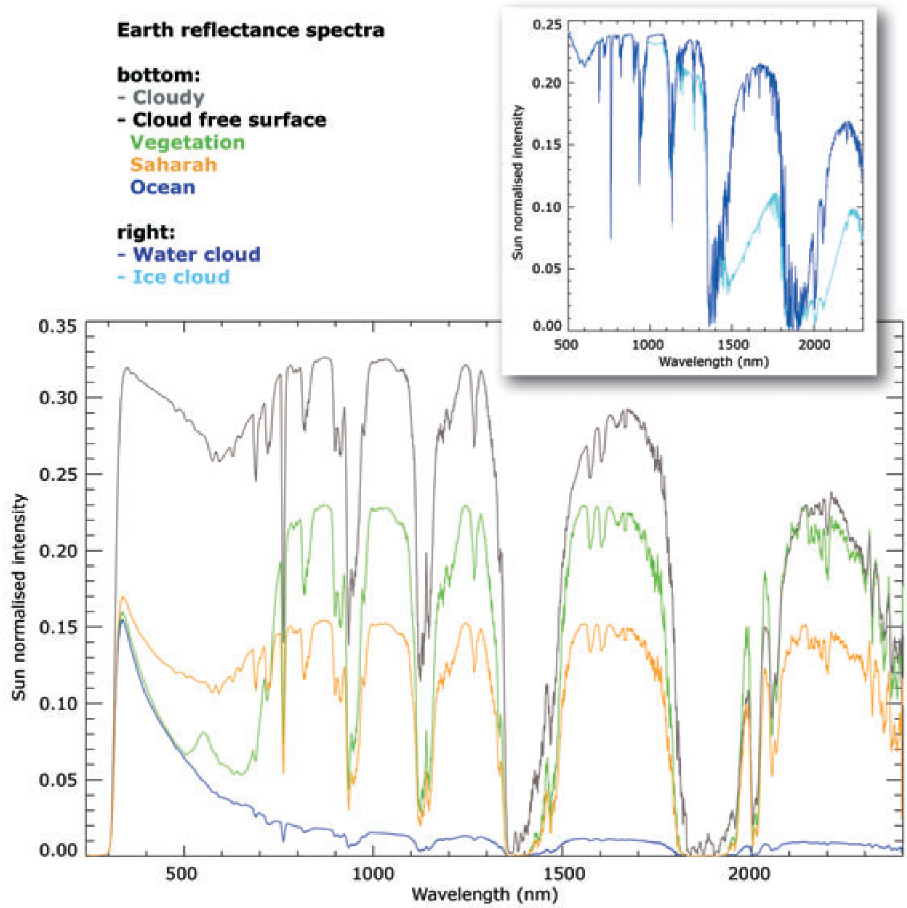

Fig. 7-7: Earth reflectance spectra (sun normalised intensity) for various cloud and surface conditions. The inset shows the variation in the reflectance spectrum due to changes in the thermodynamic state of water from liquid water to ice. The large difference in the reflectance spectrum around 1600 nm is used to derive information on the thermodynamical state of water in clouds. (graphics: IUP-IFE, University of Bremen)

Parameter	***Spectral Window (nm)***	***Retrieval Algorithm***	***Retrieval Algorithm Reference***
CF	PMD (RGB)	OCRA	*Loyola 1998*
		HICRU	*Grzegorski et al. 2004*
		SPCA	*Yan 2005*
		SPICI	*Krijger et al. 2005*
	reflectance near O_2 A-band	FRESCO	*Fournier et al. 2006*
		SACURA	*Kokhanovsky et al. 2005*
CTH	O_2 A-band	FRESCO	*Fournier et al. 2006*
		SACURA	*Kokhanovsky et al. 2005, 2006*
COT	reflectance VIS-NIR	SACURA	*Kokhanovsky et al. 2005, 2006*
CGT	O_2 A-band	SACURA	*Kokhanovsky and Rozanov 2005*
$R_{eff,cld}$	reflectance VIS-NIR	SACURA	*Kokhanovsky et al. 2005, 2006*
CPI	reflectance NIR-SWIR	SACURA	*Kokhanovsky et al. 2005, 2006 Acarreta et al. 2004b*
AAI	340 and 380		*de Graaf and Stammes 2005*
AOT	several wavelengths in the VIS	SCIA-BAER	*von Hoyningen-Huene et al. 2003, 2006*
Aerosol type	several wavelengths, combination with AATSR	SYNAER	*Holzer-Popp et al. 2002a*

Table 7-2: Atmospheric geophysical parameters and retrieval algorithms – nadir cloud and aerosol parameters.

optical thickness (albedo) are required to correct the cloud impact on the trace gas concentrations. Secondly, due to its wide spectral range and despite its relatively low spatial resolution, SCIAMACHY data enables determination of important parameters for climate research like thermodynamic phase or geometrical thickness.

Cloud Fraction (CF): In order to correct for the effect of clouds, a fast and reliable cloud fraction algorithm is required for SCIAMACHY. Nearly all cloud fraction algorithms for SCIAMACHY use the PMD measurements, as their higher temporal readout frequency translates into a higher spatial resolution as compared to data from channel 1 to 8. The basic principle of the algorithms is that cloud albedo is much higher than the Earth's surface albedo (see fig. 7-8). Therefore, a pixel that is contaminated by clouds will have a higher detector signal than one that is cloud free. Cloud fractions can therefore be determined through comparison of PMD intensities. Several derivates of cloud fraction algorithms using PMD data are currently applied to SCIAMACHY data, such as the Optical Cloud Recognition Algorithm (OCRA, *Loyola 1998*) used in the operational processing, the SCIAMACHY PMD Cloud Algorithm (SPCA, *Yan 2005*), the Heidelberg Iterative Cloud Retrieval Utilities (HICRU, *Grzegorski et al. 2004*) or the SCIAMACHY PMD Identification of Clouds and Ice/snow (SPICI, *Krijger et al. 2005*).

Cloud Top Height (CTH): CTH can be estimated from measurements in the solar backscatter spectral ranges by using the changes in the penetration depth of solar photons due to strong changes in the absorption of trace gases with known vertical distributions such as O_2 (see fig. 7-9). The idea for the CTH retrieval from O_2 A-band absorption was originally proposed by *Yamomoto and Wark (1961)*. For SCIAMACHY two algorithms are currently implemented to derive cloud top height from O_2 A-band measurements. These are the Fast Retrieval Scheme for Clouds from the Oxygen A-band (FRESCO, *Koelemeijer et al. 2001*, *Fournier et al. 2006*) and the Semi-Analytical Cloud Retrieval Algorithm (SACURA, *Rozanov and Kokhanovsky 2004*). It is worth mentioning that in addition to the O_2 A-band, there is also the option to derive CTH information from the O_2-O_2 absorption *(Acarreta et al. 2004a)* or the Ring effect *(Joiner et al. 1995, de Beek et al. 2001)*.

Cloud Geometrical Thickness (CGT): O_2 A-band absorption can also be used to obtain an estimate of the CGT *(Asano et al. 1995)*. The CGT values represent an estimate of the light absorption inside a cloud and are therefore suited reducing uncertainties in the cloud top altitude measurements. This method was applied to SCIAMACHY data by *Kokhanovsky and Rozanov (2005)*.

Cloud Optical Thickness (COT) and Effective Radius ($R_{eff,cld}$): Measurements of the Earth reflectance spectrum in the VIS or NIR range outside strong gaseous absorption bands permit derivation of the COT and Effective Radius *(Nakajima and King 1990, Platnick et al. 2003)*. *Kokhanovsky et al. (2005,*

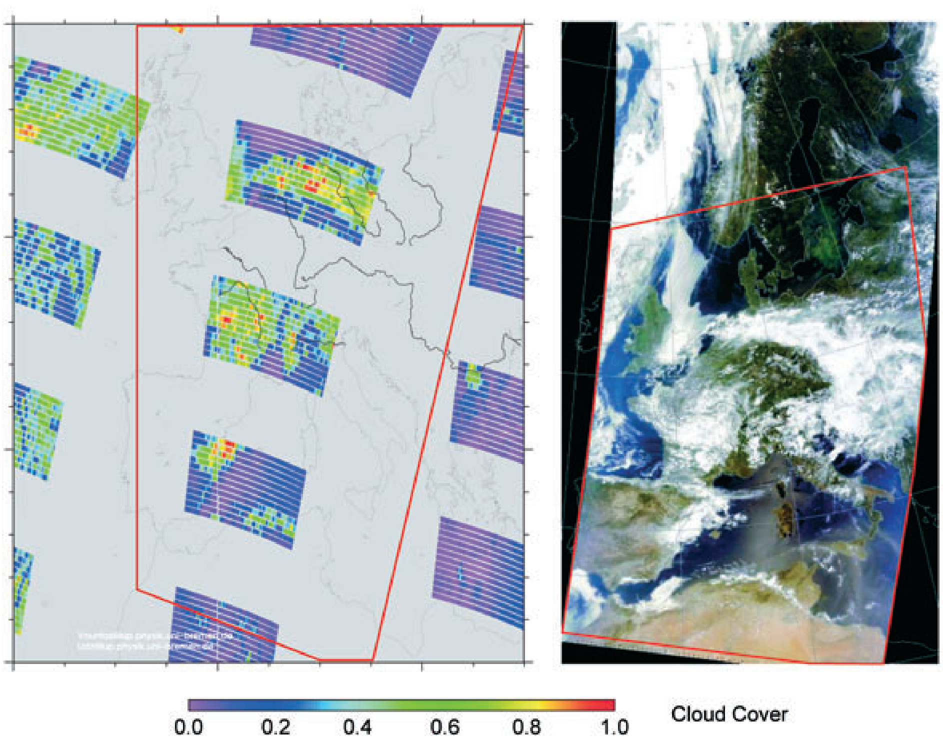

Fig. 7-8: Clouds over Europe on July 9th, 2005. Cloud coverage as seen in a RGB composite (right) from MODIS on-board TERRA and cloud fraction (left) determined with OCRA using SCIAMACHY PMD data (images: IUP-IFE, University of Bremen and Dundee Satellite Receiving Station)

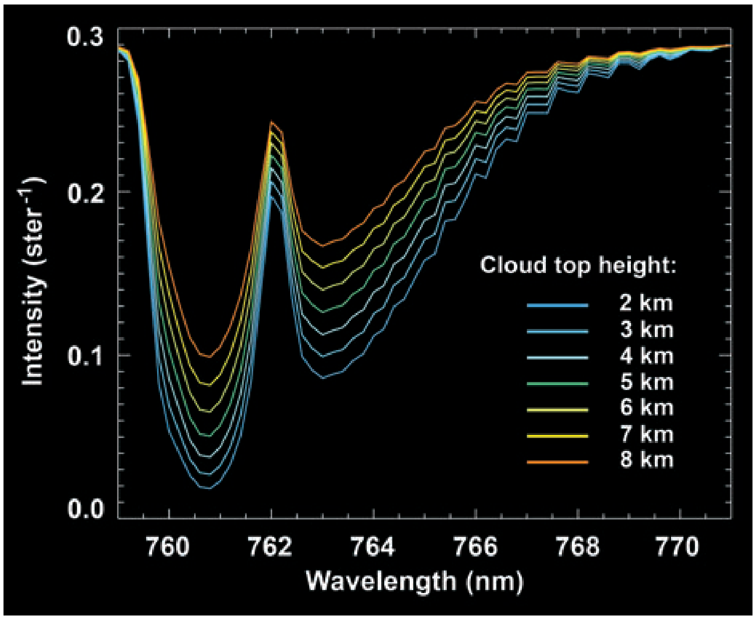

Fig. 7-9: The top-of-atmosphere reflectance in the O_2 A-band as a function of cloud top height. (graphics: IUP-IFE, University of Bremen)

In the GOME/SCIAMACHY data processing environment mainly two cloud retrieval algorithms are exploited. One is FRESCO, which uses measurements inside and outside the O_2 A-band (758-778 nm). FRESCO is developed for cloud correction of trace gas retrievals, like O_3 and NO_2. It simultaneously retrieves an effective Cloud Fraction (CF_{eff}) and an effective Cloud Top Height (CTH_{eff}) assuming that the cloud can be represented as a bright Lambertian surface with a fixed albedo value of 0.8. The second cloud algorithm employed in the operational processing is the combination of OCRA with SACURA. OCRA delivers cloud fraction as input for SACURA to determine CTH and COT. In addition, an improved version of SACURA delivers cloud geometrical thickness, effective radius and the cloud thermodynamical state *(Kokhanovsky et al. 2005, 2006)*.

2006) applied the method to SCIAMACHY data. In the case COT and $R_{eff,cld}$ are known for a liquid water cloud, the liquid water path can be estimated.

Cloud Phase Index (CPI): SWIR reflectance measurements are also suitable for obtaining the cloud phase index CPI *(Knap et al. 2002, Acarreta et al. 2004b, Kokhanovsky et al. 2005, 2006)*, as the dependence of the single scattering albedo on the particle size is different for liquid water and ice.

Tropospheric Aerosol Parameters

Aerosols are characterised by high spatial or temporal variability and a mixture of chemically and physically different particles, dependent on their origin *(Pöschl 2005)*. Detection of aerosol by spaceborne instruments utilise their effect on the reflected solar radiation observed at the top of the atmosphere. Contributions from Earth's surface reflections (see fig. 7-7) and atmospheric gases (see fig. 7-3) need to be separated

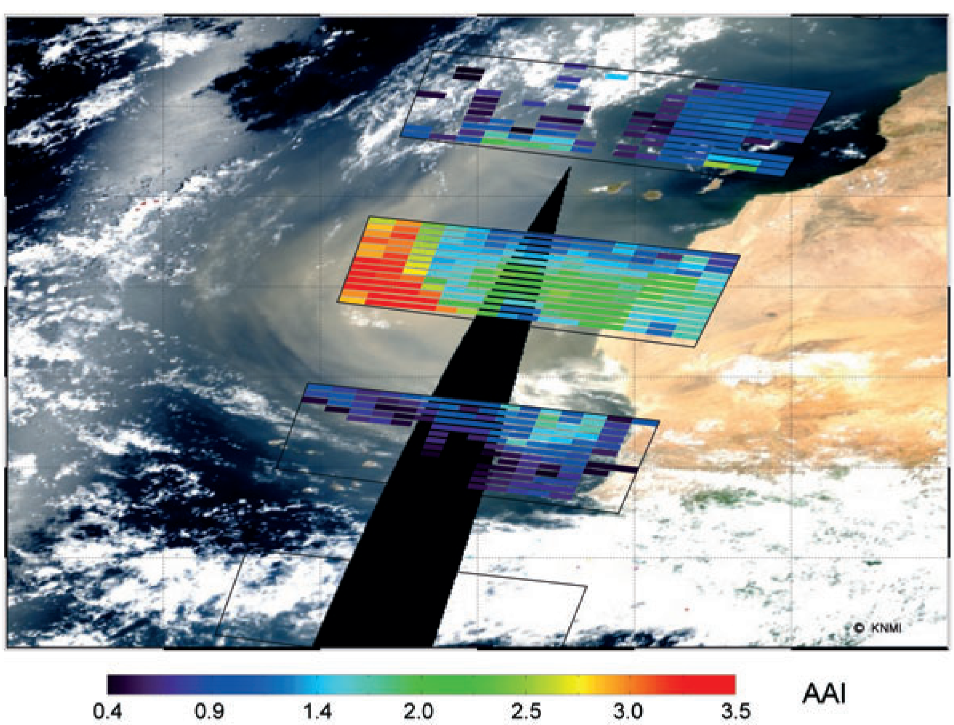

Fig. 7-10: Saharan desert dust outbreak to the Atlantic on July 25th, 2004. Shown are the SCIAMACHY AAI at 9:15 UTC of that day overlaid on a MODIS RGB picture, acquired around 11:10 UTC (right side of the plot) and 12:50 UTC (left side of the plot). High SCIAMACHY AAI values coincide with the dust plume, visible as a yellow haze on the MODIS image. (image: M. de Graaf, KNMI)

using available information on the surface properties and the effects of gases. Thus the signatures of aerosols can be derived and can be used to retrieve aerosol properties.

Most of currently existing aerosol retrieval algorithms are aimed to determine the Aerosol Optical Thickness (AOT), i.e. columnar extinction by aerosol particles and their spectral behaviour. All higher level aerosol parameters (aerosol concentration, effective radius and others) can be derived from the magnitude and the spectral behaviour of the AOT. Thus, the spectral AOT may be regarded as the key parameter concerning retrieval of other aerosol properties. It is extracted by fitting modelled reflectance spectra to the measured reflectance spectra. This approach needs careful constraints based on the knowledge on molecular scattering, absorption and the surface reflectance *(von Hoyningen-Huene et al. 2003)*. The first application to SCIAMACHY data is found in *von Hoyningen-Huene et al. (2006)*.

From UV wavelengths below 400 nm the Absorbing Aerosol Index (AAI) can be derived. The AAI indicates the presence of absorbing aerosol, mainly caused by strong events like Sahara dust outflows or biomass burning (see fig. 7-10). Initially developed as an error indicator for ozone retrieved from TOMS data *(Herman et al. 1997)*, the AAI is the aerosol quantity with the longest data record. The AAI is derived as the residual between the measured reflectance from an atmosphere enriched with aerosols and the simulated reflectance of an atmosphere with only Rayleigh scattering, absorption by molecules, plus surface reflection and absorption *(de Graaf and Stammes 2005)*. Such an algorithm using SCIAMACHY data at 340 nm and 380 nm delivers meaningful AAI values, in case properly calibrated spectra are used *(de Graaf and Stammes 2005)*.

The combination of SCIAMACHY spectral information with data from high resolution images from AATSR on ENVISAT, will enable the derivation of the aerosol type information, beside the AOT. The synergistic method SYNAER *(Holzer-Popp et al. 2002a, 2002b)* can be applied to exploit SCIAMACHY together with AATSR to derive aerosol type information.

7.4 Inversion Theory

The forward modelling described earlier in chapter 7.1 is commonly employed to simulate a measured quantity, e.g., intensity of the radiation, for a predefined state of the atmosphere. Contrary to this, the objective of inversion problems is to retrieve certain characteristics of the atmospheric state – for example trace gas concentration profiles – based on the measured quantities. These can be for example the solar radiance transmitted through the Earth's atmosphere in the occultation geometry or the radiance scattered by the Earth's atmosphere or reflected by the surface in the limb or nadir geometry.

The parameters to be retrieved from the measurements are represented by a *model state vector x*. For example, for trace gas vertical profile retrieval, the model state vector contains the number densities of atmospheric constituents defined at discrete altitude levels. Each state vector can be mapped to the measurement space by means of the forward model operator F to obtain the corresponding measurement vector y, i.e., for each atmospheric state described by vector x an appropriate measured quantity y can be simulated using a radiative transfer model as the forward model (see fig. 7-11).

In the case of SCIAMACHY occultation or limb measurements, the measured quantities are represented by a set of intensities measured at different tangent heights in selected spectral windows. Taking into account that measurements are made to a finite accuracy, a measurement error ε has to be considered which is commonly assumed to be normally distributed with mean zero and known error covariance matrix S_y. Thus, the relationship between the model state vector and the measurement vector can be written as (equ. 7-7)

$$y = F(x) + \varepsilon$$

In order to solve the inverse problem, this non-linear relationship in equ. 7-7 has to be linearised expanding the forward model operator, F, as a Taylor series about a guessed value x_0 of the solution. Ignoring the higher-order terms one obtains (equ. 7-8)

$$F(x) \approx F(x_0) + \left.\frac{\partial F}{\partial x}\right|_{x_0} (x - x_0) = y_0 + K_0 (x - x_0)$$

Here, K_0 is the linearised forward model operator. In the discrete representation the linearised forward model operator is given by the weighting function matrix describing the sensitivity of the measured quantities to the variation of the atmospheric parameters at different altitude levels. This weighting function matrix is calculated with the radiative transfer model.

Atmospheric inversion problems are commonly 'ill-posed'. Thus, additional constraints need to be

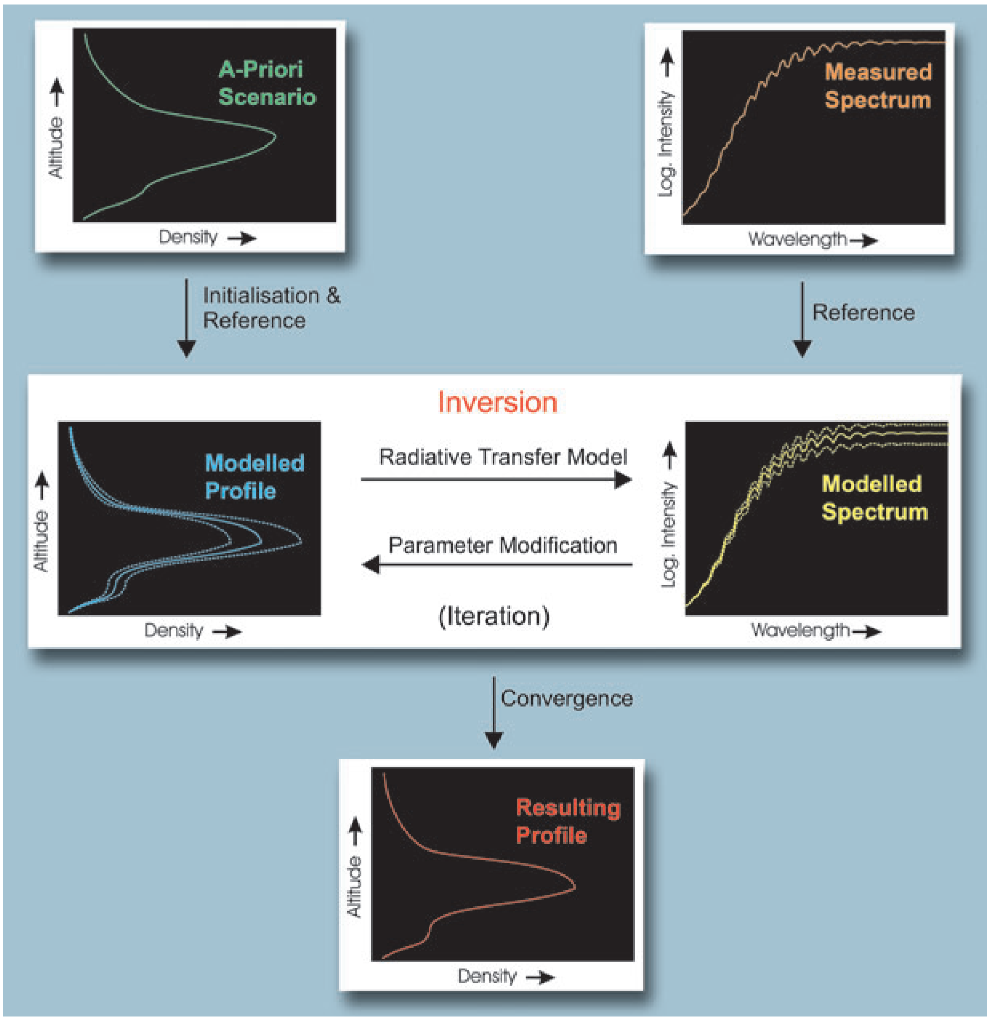

Fig. 7-11: The principle of inversion for the retrieval of geophysical parameters. For further details see the text. (graphics: IUP-IFE, University of Bremen)

introduced to determine a geophysical solution from the set of mathematically allowed solutions. Most commonly, the methods of statistical regularisation, as described e.g. by *Rodgers (2000)* are applied, i.e., the maximum likelihood condition, a priori value of the solution, x_0, and its covariance matrix, S_a, are employed to solve the inversion problem. In this case the solution is found by minimising the following quadratic form (equ. 7-9)

$$\left\|(y-y_0)-K_0(x-x_0)\right\|^2_{S_y^{-1}}+\left\|x-x_0\right\|^2_{S_a^{-1}}\rightarrow \min$$

This results in (equ. 7-10)

$$x_{n+1}=$$
$$x_0+\left(S_a^{-1}+K_n^T S_y^{-1}K_n\right)^{-1}K_n^T S_y^{-1}\left((y-y_n)-K_n(x_0-x_n)\right)$$

where subscripts n and $n+1$ denote the number of the iteration. The measurement error covariance matrix, S_y, is usually assumed to be diagonal, i.e. no correlation between measurement errors at different wavelengths or different tangent heights is considered.

In the retrieval of the vertical distributions of the atmospheric species the *a priori* covariance matrix, S_a, is commonly chosen as a block diagonal matrix, i.e. vertical distributions of different atmospheric trace gases are assumed to be uncorrelated. The diagonal elements of S_a represent the variances of the vertical distribution of atmospheric trace gases, σ, which e.g. can be derived from a climatology.

The quality of the obtained solution is characterised by the *a posteriori* covariance matrix (equ. 7-11)

$$S=\left(K^T S_y^{-1}K+S_a^{-1}\right)^{-1}$$

and by the averaging kernels (equ. 7-12)

$$A=\frac{\partial x}{\partial x_{true}}=\left(K^T S_y^{-1}K+S_a^{-1}\right)^{-1}K^T S_y^{-1}K$$

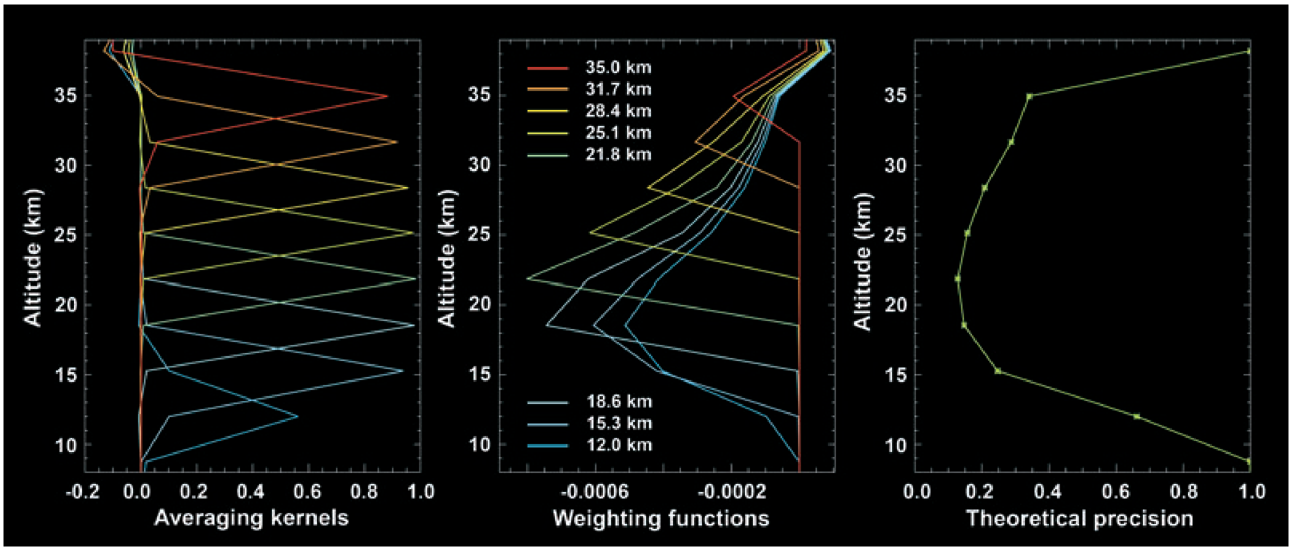

Fig. 7-12: Averaging kernels (left), weighting functions at 338.6 nm (middle), and theoretical precision (right) for BrO vertical profile retrievals from SCIAMACHY limb measurements. (graphics: IUP-IFE, University of Bremen)

characterising the response of the retrieved solution to the variation of the true atmospheric state. The root squares of the diagonal elements of the *a posteriori* covariance matrix are referenced to as the theoretical precisions.

Employing the averaging kernels, the retrieved solution, x, can be related to the true solution, x_{true}, as (equ. 7-13)

$$x = x_0 + A(x_{true} - x_0)$$

i.e., if the model state vector represents a vertical profile of an atmospheric trace gas, the retrieved values at each altitude are expressed as the sum of the *a priori* value at this altitude and of the deviation of the true profile from an a priori profile smoothed with the associated row of the averaging kernel matrix. For an ideal observing system, A is a unit matrix. In reality, the rows of the averaging kernel matrix are peaked with a finite width, which can be regarded as a measure of the vertical resolution of the retrieved profile.

7.5 Application of Inversion Theory to Limb Retrieval

For the retrieval of the vertical distributions of atmospheric species from the measurements performed by SCIAMACHY the so called *Global Fit* technique is an effective way of implementing the inversion. The measurement vector contains the logarithms of the radiances in all selected spectral points and at all line-of-sights, both for limb and occultation geometry, referenced to an appropriate irradiance spectrum. In the limb viewing geometry, the irradiance spectrum can be replaced by a limb measurement at an upper tangent height. Due to this normalisation the retrieval is relatively robust with respect to the radiometric calibration. In addition, the normalisation significantly reduces the sensitivity of the retrievals with respect to ground albedo and cloud cover. Commonly, before the main inversion step, a pre-processing is performed intended to correct for possible misalignment in the wavelength calibration and account for known atmospheric corrections such as the Ring effect. If required, a polynomial can be subtracted from all relevant spectra involved accounting for both missing or inappropriate instrument calibration and unknown scattering properties of the atmosphere.

To illustrate the limb inversion in practice, fig. 7-12 shows an example of averaging kernels, weighting functions at 338.6 nm, and theoretical precision typical for BrO vertical profile retrieval from SCIAMACHY limb measurements. These results were obtained using the limb measurement at a tangent height of 38.5 km as a reference spectrum. As can be seen in the figure, the peak values of the averaging kernels are close to 1.0 only at tangent heights above 15 km. The peak value of about 0.55 at 12 km altitude indicates an increased dependence of the retrieved BrO amount at this altitude on BrO amount at neighboring altitude levels and *a priori* information. Looking at the width of the averaging kernels, the height resolution of the measurements can be estimated to about 3 km, close to the geometrical resolution of the instrument. The weighting functions in the middle panel exhibit relatively sharp peaks near the tangent height down to 18 km tangent height, whereas at all lower tangent heights the weighting functions peak at about 18 km altitude. Nevertheless, the BrO amounts down to 12 km can be retrieved due to different shapes of the corresponding weighting functions. In accordance with the averaging kernels, the theoretical precision of the BrO vertical profile retrieval shown in the left panel has reasonable values of 10-40% only above 14 km altitude and rapidly decreases below indicating the low information content in the measurements below 14 km.

To date, such type of retrieval algorithm and associated derivates has been used to obtain stratospheric profiles of O_3, NO_2 *(Bracher et al. 2005, Sioris et al. 2004)* and BrO *(Rozanov et al. 2005b)* from SCIAMACHY limb scattering profiles. This type of inversion algorithm was also applied and used to derive trace gas concentrations from lunar *(Amekudzi et al. 2005a, 2005b)* and solar occultation *(Meyer et al. 2005)* measurements. It is interesting to note that a similar approach as described above can also be applied to retrieve trace gas information from nadir measurements, as for example demonstrated for the ozone profile retrieval from GOME nadir measurements *(Munro et al. 1998, Hoogen et al. 1999)*.

All the applications listed above use a continuous spectral range to derive the trace gas information. Another group of limb inversion algorithms employs discrete spectral points in and outside strong trace gas absorption bands for the retrieval of vertical profiles. Retrieval algorithms utilising the difference in absorption between the centre and wings of the ozone Chappuis and Huggins bands were devised by *Flittner et al. (2000)*. In a first step the limb radiance profiles are normalised with respect to a reference tangent height between 40 and 45 km. For the SCIAMACHY O_3 Chappuis band retrieval *(von Savigny et al. 2005a)*, the normalised limb radiance profiles are divided by the limb radiance profile at a non-absorbing wavelength and then analysed in an optimal estimation scheme to retrieve the stratospheric O_3 profiles. Retrievals in the O_3 Chappuis band allow

Parameter	**Spectral Window (nm)**	**Layer**	**Quantity**	**Retrieval Algorithm Reference**
O_3	525, 600, 675	stratosphere	profile	*von Savigny et al. 2005a*
	525-590			*Doicu et al. 2002, Doicu 2005*
	240-310 (selected wavelengths)	mesosphere	profile	*Rohen et al. 2006*
	520-595	stratosphere	profile sun occultation	*Meyer et al. 2005*
	510-560	stratosphere	profile moon occultation	*Amekudzi et al. 2005a*
NO_2	425-450(70)	stratosphere	profile limb	*Rozanov et al. 2005b* *Sioris et al. 2004* *Doicu et al. 2002, Doicu 2005*
	420-460	stratosphere	profile sun occultation	*Meyer et al. 2005*
	430-460	stratosphere	profile moon occultation	*Amekudzi et al. 2005a*
NO_3	610-680	stratosphere	profile moon occultation	*Amekudzi et al. 2005b*
BrO	335-360	stratosphere	profile	*Rozanov et al. 2005b* *Dorf et al. 2005*
OClO	365-389	stratosphere	profile	
NLC	265-300	mesosphere	indicator, particle radius	*von Savigny et al. 2004a*
PSC	750, 1090	stratosphere	indicator	*von Savigny et al. 2005b*
$T_{mesopause}$	1515-1550	mesosphere	nighttime temperature at mesopause	*von Savigny et al. 2004b*

Table 7-3: Atmospheric geophysical parameters and retrieval algorithms – limb and occultation.

extraction of stratospheric O_3 profiles for altitudes between about 12-14 and 40 km. The retrieval range is limited at lower altitudes because the atmosphere becomes optically thick with respect to Rayleigh scattering and/or O_3 absorption. Above about 40 km the O_3 absorption signatures become too weak to be observed. However, normalised limb radiance profiles in the O_3 Hartley and Huggins bands can also be used without further wavelength pairing for the derivation of ozone profiles in the upper stratosphere and lower mesosphere *(Rohen et al. 2006)*. The O_3 retrievals may be extended up to at least 65 km since the absorption cross sections in the Hartley and Huggins bands are significantly larger than in the Chappuis band.

The wide variety of retrieval algorithms currently applied to SCIAMACHY limb and occultation data are summarised in table 7-3, together with their corresponding references.

7.6 Derivation of Tropospheric Information

Of major scientific – and public – interest are distributions of trace gases in the troposphere. Two cases need to be distinguished:

- Constituents with the majority of the atmospheric amount residing in the lower troposphere (e.g. CO, CH_4, CO_2, HCHO, SO_2, H_2O): The total column derived from UV-VIS and SWIR solar backscatter measurements with the techniques derived in chapter 7.3 directly represents the tropospheric column amount including the boundary layer under cloud free conditions.
- Trace gases with comparable column amounts in the troposphere and stratosphere (e.g. BrO, NO_2) or with the stratospheric amount dominating the total column (e.g. O_3): Additional techniques have to be applied to separate tropospheric and stratospheric concentrations.

For the latter case dedicated techniques are required to separate the tropospheric and the stratospheric concentrations. One approach is to use measurements over a clean air region as a background, the so-called *Reference Sector Method* (see below). In addition, SCIAMACHY's unique limb/nadir matching capabilities (see chapter 4) provide a nearly simultaneous stratospheric profile measurement for each nadir measurement. In that respect, SCIAMACHY is clearly superior to its predecessor GOME which obtained measurements of the same species in the UV-VIS range but only in nadir geometry.

Reference Sector Method

The Reference Sector Method, also referred to as *Tropospheric Residual Method (Velders et al. 2001, Richter and Burrows 2002, Martin et al. 2002)* allows the separation of tropospheric and stratospheric contributions to the total NO_2 content under the assumption of a stable – both spatial and temporal – NO_2 distribution over the clean, free Pacific Ocean. It is assumed that the stratospheric NO_2 distribution is homogeneous with longitude. Then the tropospheric NO_2 is primarily the difference between the total column measured over a polluted area and the total column measured over the clean Pacific Ocean. This technique needs no stratospheric profile information and can therefore be applied to generate a consistent GOME – SCIAMACHY tropospheric NO_2 data set (see chapter 10).

Limb/Nadir Matching

One important area of uncertainty in the determination of the tropospheric column concentration from solar backscatter nadir measurements is the error introduced by estimating the stratospheric column concentration *(Boersma et al. 2004)*. To improve on this topic, it is required to use the measured stratospheric column above the ground scene of interest. SCIAMACHY with its limb/nadir matching measurement mode provides radiances from the same volume of air in limb and nadir geometry since 2002. This allows inference of vertical stratospheric concentration profiles directly over the region of the nadir measurement. Integrating these profiles from the tropopause upwards yields the measured stratospheric column above the target area while the collocated nadir measurement provides the total column amount. The tropospheric column is then – very briefly speaking – determined as the difference between the total and the stratospheric column. An initial application of this approach to derive tropospheric NO_2 was presented in *Sierk et al. (2006)*. The method described here is unique in the sense that the information on the stratospheric content is taken directly from the collocated limb measurement and no other assumptions (longitudinal homogeneity) or an estimate of the stratospheric column from a model or from data assimilation are necessary.

7.7 Data Assimilation and Value Added Products

Data assimilation generates synoptic trace gas fields from asynoptic spaceborne measurements. This enables the derivation of interpolated concentration

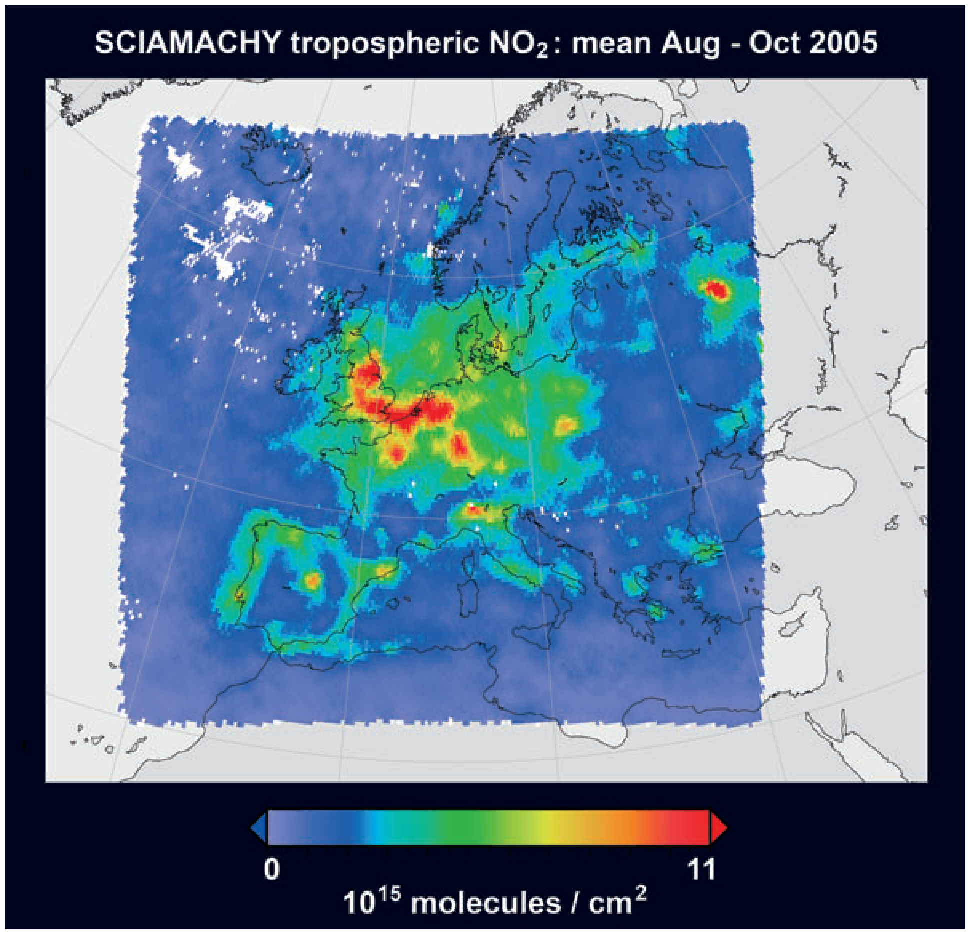

Fig. 7-13: Mean tropospheric NO_2 vertical column densities over Europe as derived from SCIAMACHY for August to October 2005 with the DLR-DFD assimilation approach. (image: T. Erbertseder, DLR-DFD)

fields, e.g. to separate tropospheric and stratospheric contributions, as well as information about transport mechanisms. Several assimilation schemes are applied to SCIAMACHY measurements to combine stratospheric modelling and nadir column data. They produce results usually referred to as *Value Added* products.

Tropospheric Trace Gases – the NO_2 Example

NO_2 permanently resides in the stratosphere and shows significant amounts in the troposphere near source areas. First, the stratospheric and tropospheric parts of the column need to be separated and subsequently, a tropospheric airmass factor needs to be applied to the tropospheric slant column. At KNMI, in collaboration with BIRA/IASB, a data assimilation system was applied to NO_2 to derive the stratospheric part of the slant column by assimilation of observed slant columns in a chemistry-transport model *(Eskes et al. 2003)*. This results in a stratospheric analysis consistent with the observations as well as with variations observed in the stratosphere that are due to the atmospheric dynamics and chemical reactions. The tropospheric NO_2 slant column is then extracted by subtracting the assimilated stratospheric slant column from the retrieved total slant column.

In a similar way the stratospheric NO_2 slant column density, exactly for the SCIAMACHY overpass time, is derived from the stratospheric chemistry transport model ROSE at DLR-DFD. To avoid a bias, the modelled analyses are scaled to 'clean conditions' over the Pacific Ocean. The tropospheric NO_2 slant column is then extracted by subtracting the modelled stratospheric slant column from the retrieved total slant column. Fig. 7-13 shows the resulting tropospheric NO_2 distribution over Europe. The tropospheric NO_2 distributions can be further improved by using NO_2 profile shapes estimated by air quality models like EURAD. In this case also properties of clouds, aerosols and the surface have to be taken into account.

Stratospheric O_3

Assimilated total column and stratospheric profile fields are ideally suited for applications such as scientific studies of the evolution of the ozone layer and of special events (e.g. ozone hole or low ozone episodes) or inter-comparisons with models (e.g. study of dynamical and chemical processes). Since assimilated fields are globally available, comparison with independent observations can be performed without space/time mismatches.

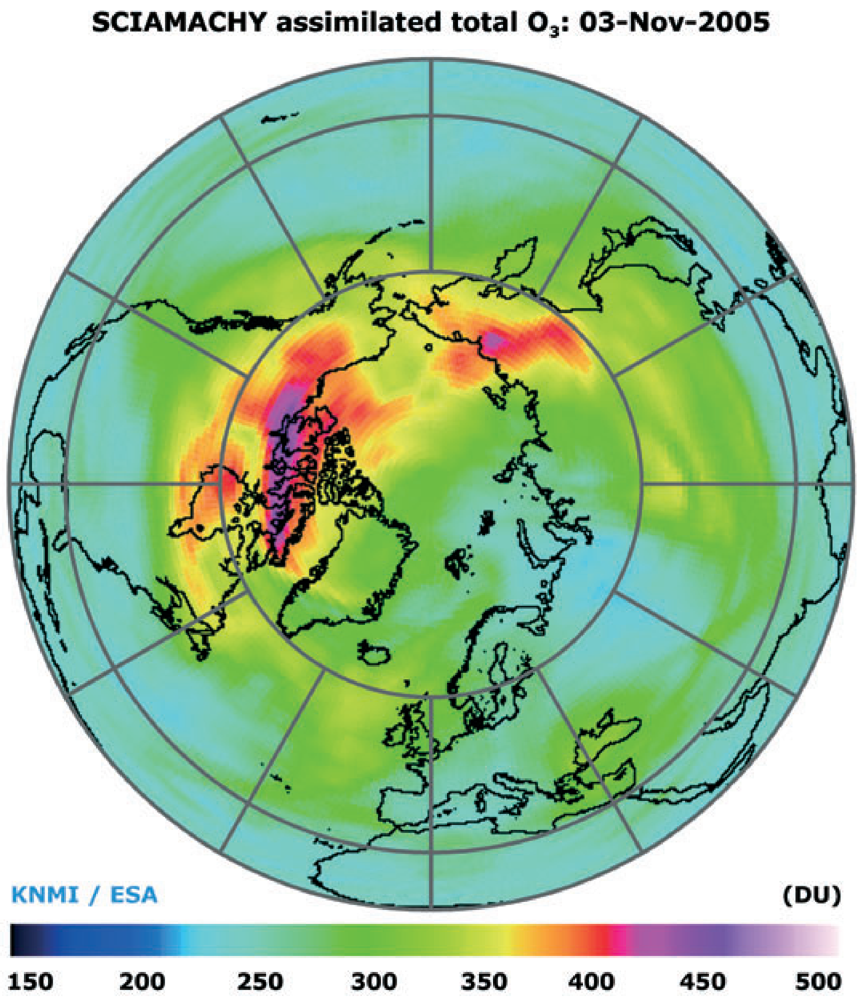

Fig. 7-14: A forecasted North Pole view of the assimilated total ozone column field for November 3rd, 2005 at 12:00 UTC based on SCIAMACHY data. (image: KNMI/ESA)

Stratospheric O_3 is also of particular interest as it can be assimilated into operational weather forecasts and improves the model representation of stratospheric wind fields and thereby the quality of the forecast. Since forecast services are provided on short timescales, the availability of near-realtime O_3 data is essential. Total columns of ozone can be derived from SCIAMACHY measured backscatter reflectivities in near-realtime (*Eskes et al. 2005*). These ozone columns serve as an input for the assimilation analysis and a subsequent forecast of how the stratospheric ozone layer will develop in the upcoming 9 days. The assimilation yields a complete picture of the global ozone distribution (see fig. 7-14). Within the error margins of both model and observations it is consistent with observations and our knowledge of atmospheric transport and chemistry (*Eskes et al. 2002, 2003*). SCIAMACHY ozone columns are currently also assimilated operationally in the numerical weather prediction model of the ECMWF. Several centres use the ozone forecasts for UV radiation predictions (see chapter 10.5).

To further analyse and quantify atmospheric processes such as ozone depletion or ozone loss rates, an optimal combination of models and asynoptic or heterogeneously distributed observations is essential. By using for example the ROSE transport model, SCIAMACHY observations of O_3, NO_2, OClO and BrO can be assimilated in order to derive a consistent global chemical analysis of the stratosphere.